

Predicting effective constitutive constants for woven-fibre composite materials

Jonas T. da Rocha¹, Tales V. Lisbôa², Rogério J. Marczak¹

¹*Mechanical Engineering Department, Federal University of Rio Grande do Sul
Rua Sarmento Leite, 425, Porto Alegre, RS, Brazil*

jonas.tieppo@ufrgs.br

²*Mechanics and Composite Materials Department, Leibniz Institute of Polymer Research
Hohe Str. 6, 01069 Dresden, Germany*

tales-lisboa@ipfdd.de

Abstract.

A meso-scaled finite element model is developed aiming at the study the mechanical properties of woven-fibre composites regarding different weave pattern. A Representative Volume Element (RVE) is constructed and the Uniform Displacement Boundary Conditions (UDBC) are applied in order to obtain the stiffness tensor of such composites. Two different types of woven-fibre composites are evaluated by the introduced model - E-glass/Vinylester plain-weave and 2/2 Twill E-glass/Epoxy. The results from computational homogenization are compared to both experimental and numerical works from literature, showing good agreement. It is verified that the boundary conditions applied to the RVE play a significant role in the homogenization results.

Keywords: Woven composites, Computational homogenization, Finite Element Method, Heterogeneous structures

1 Introduction

The woven-fibre modelling, aiming at mechanical properties, can be divided in two main approaches: numerical methods and analytical solutions. Regarding to analytical solutions, Ishikawa [1] and Ishikawa and Chou [2] proposed the one-dimensional *Mosaic Model*, the first well-known solution for woven-fiber composites, primarily for satin weaves and hybrid composites. The *Mosaic Model* treats the woven either as an parallel or serial asymmetric cross-ply laminates assemblage. It leads to *upper* and *lower* bounds of stiffness matrix. This first approach has the disadvantage of neglecting interweaving effects, as the undulation of warp and fill strands is not modelled. With *Fiber Undulation Model*, Ishikawa and Chou [3] overcame this *Mosaic Model* disadvantage. This last model was idealized to predict plain-weave composites, being an extension of *Mosaic Model*.

Further developments were made by Sankar and Marrey [4] who presented the *Selective Averaging Method* (SAM), which dealt with three-dimensional and two-dimensional textile composites and proposed a formulation to estimate stiffness and thermal expansion coefficients. Three-dimensional composites were divided into three microstructure levels: *unit cell*, *slice* and *element*, which correspond, respectively, to *macro*, *meso* and *micro* stiffness. In order to obtain the coefficients of the stiffness tensor, it is assumed macro uniform strain states in the entire domain - six states in total, encompassing each strain alone. This macro strain state is assumed to be approximately equal in *meso* and *micro* scales, permitting an easy integration of the stiffness between *micro* and *meso-scales*. Later, the *meso* scale *slices* are averaged assuming an *isotress* condition. Finally, the *macrostress*s are averaged in the volume, what lets to express each column of the stiffness matrix in terms of *meso* and *micro* strains. In case of two-dimensional composites, the textile composite is divided into repeating cells in in-plane directions, being modelled as an homogeneous Kirchoff's plate in *macro-scale*. The procedure to estimate the plate stiffness coefficients is analogous to the three-dimensional case.

Scida [5] presented a model based in Classical Laminate Theory to predict mechanical properties of woven-fibre composites (hybrid and non-hybrid). This model, called MESOTEX (Mechanical Simulation of Textile), treats the woven composite as a combination of two homogeneous phases: orthotropic strands and isotropic matrix. The undulation of strands are geometrically described by sinusoidal functions, while in other parts the path are

considered straight. Similar approach was done by Ming [6], who proposed a method to estimate mechanical properties for woven and braid composites. In it, the composite was divided into subelements and it was applied an *isostrain* condition in each division so as to obtain their stiffness. The subelements corresponded to four layered unidirectional composites, with two inner layers being the homogenized strands, and the two outer layers matrix. Later, in order to assemble the subelements, *isotress* condition is applied.

The analytical models are really useful for a fast estimation of the (homogenised) mechanical properties. However, numerical models can evaluate stresses distributions along the geometry, therefore giving insights about the mechanical performance of the composite. One of the most important aspects of this approach is the correct modeling of the composite geometry. Barbero [7] used photomicrograph measurements to model geometry correctly. The photomicrograph data was fitted with sinudoisal functions, and finally the geometry was totally built in a commercial CAD. Although such type of approach is valid, some composite-specialized software were developed in the recent years. Verpoest and Lomov [8] developed *WiseTex*, an software able to calculate 2D and 3D composites, which composite geometry is described by analytical models. Furthermore, Ling [9] presented *TexGen*, and open-source composite modelling software. *TexGen* can model 2D and 3D woven fabrics, as well any user-defined geometry, as the software accepts Python scripts to define the geometry paths.

In this article, *TexGen* will be used to model the geometry of woven-fibre composites, with data available in Scida [10]. Two woven-fibre classes will be treated - E-glass/vynilester plain-weave and E-glass/Epoxy 2/2 Twill-weave. The homogenization is performed by choosing a set of boundary conditions that respect the *Hill's Energy Condition*. Hence, *Uniform Displacement Boundary Conditions* (UDBC) is applied, which leads to a linear system that allows the complete determination of the homogenized stiffness matrix of the woven-fibre composite.

2 3D finite element modeling of RVE

2.1 Geometric Modelling

Woven-fibre composites geometry exhibits periodicity, which allows the designer to analyse only a representative element volume (RVE) in order to obtain the mechanical behaviour of the entire component / domain. The Repetitions Unity Cell (RUC) can then be used to construct such RVE. Fig. 1 presents two examples of RUCs that are also studied in the present work.

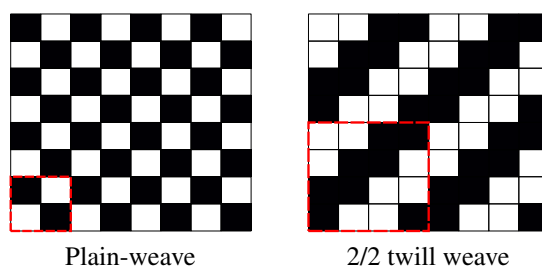


Figure 1. Weave pattern draft and RUC adopted (dashed red square)

The RVE geometry is built in *TexGen* [9, 11], using composite data from Scida [10] (See Table 1). In the model, there are three volume fractions to be considered, as showed in Fig. 3. The first one, V_0 , refers to *dry volume fraction*. This is the volume occupied by fibers inside the whole composite volume. The second volume fraction, V_g , *meso-scale volume fraction*, is the portion occupied by strands (fills and warps with impregnated resin). By last, the *strand volume fraction*, V_s , is the volume occupied by fibers in strands. Figure 2 shows the geometry created in *TexGen*.

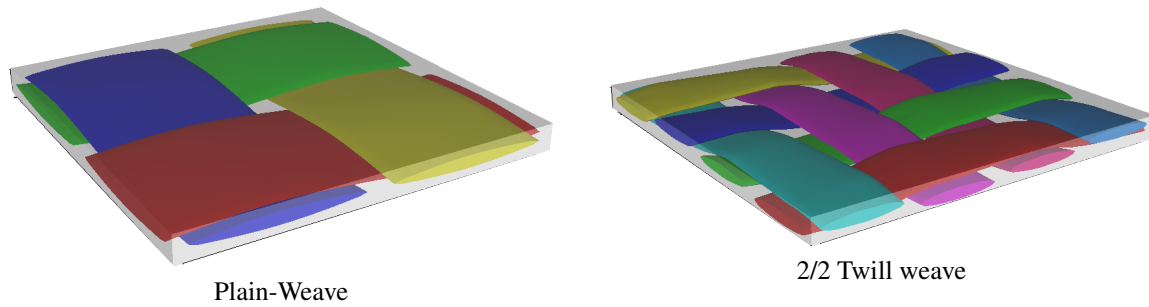


Figure 2. Weave-fibre composite models created in TexGen [9, 11]

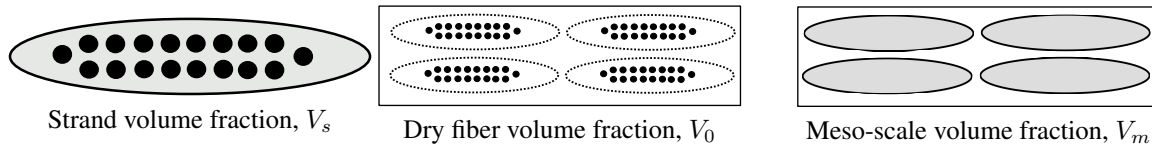


Figure 3. Composite Volume fractions

Table 1. Weave geometry parameters, Scida [10]

Material	Weave class	Strand width (mm)	Comp. thickness (mm)	Yarn Spacing* (mm)	V_0	V_s	V_m^{**}
E-glass/Vinylester	Plain weave	0.6	0.1	0.625	0.55	0.8	0.6875
E-glass/Epoxy	2/2 twill weave	0.83	0.2275	1	0.38	0.75	0.5067

*This parameter does not appear in Scida [10]. However, it is a mandatory parameter for TexGen [9, 11]. Therefore, the values used in this work were selected to reproduce experimental V_m closest as possible.

**Calculated by $V_s = \frac{V_0}{V_m}$, as stated in Barbero [7].

The correct V_m representation of the composite might be a difficult task in woven-fibre analysis. In TexGen [9, 11], if one performs the model creation, a default increase of 10% of matrix in height is applied to the composite, creating a shallow film of matrix in lower and upper faces of the composite. Such additional matrix volume incurs that V_m decreases in the model. If one constricts such resin surplus, the thickness of matrix above (and below) strands would become excessively thin, requiring a finer mesh to avoid errors in modeling. As a consequence, the V_m considered in the presented model does not agree with experimental values. Following Barbero [7] methodology, one needs to carry out a *meso scale volume fraction correction*. Namely, the Compliance Matrix is corrected through eq. (1).

$$[S] = [S]^\alpha \frac{V_m^m}{V_m^\alpha} \quad (1)$$

where V_m^m and V_m^α correspond to experimental and model meso scale volume fractions, respectively, and $[S]^\alpha$ defines the compliance matrix $[S]$ prior eq. (1) application. The table 2 shows the V_m obtained in this work and the correction factor applied.

Table 2. V_m in TexGen [9, 11] and V_m correction

Material	Weave class	V_m^α	$\frac{V_m^m}{V_m^\alpha}$
E-glass/Vinylester	Plain weave	0.589	1.165
E-glass/Epoxy	2/2 twill weave	0.498	1.017

2.2 Boundary conditions

The Average Strain Theorem establishes an equivalence between a boundary condition as showed in eq. (2) and strain average in the volume, as showed in Zohdi [12]. Such condition is known as *uniform displacement boundary conditions*¹(UDBC), in which ε_{ij}^A denotes an *strain state applied*, and x_{ij} an position vector. If the coordinate system is in the geometrical center of the body with dimensions $(2a_1, 2a_2, 2a_3)$, the Fig. 4 is a representation of a uniform strain in *pure extension*. This type of boundary condition satisfies the *Hill's Energy Condition*, as stated in Zohdi [12], which means that the model presents an equivalence between macro and micro energy measurements, being a necessary condition for a heteronegenous composite homogenization.

$$u|_{\partial V} = \varepsilon_{ij}^A x_j \quad (2)$$

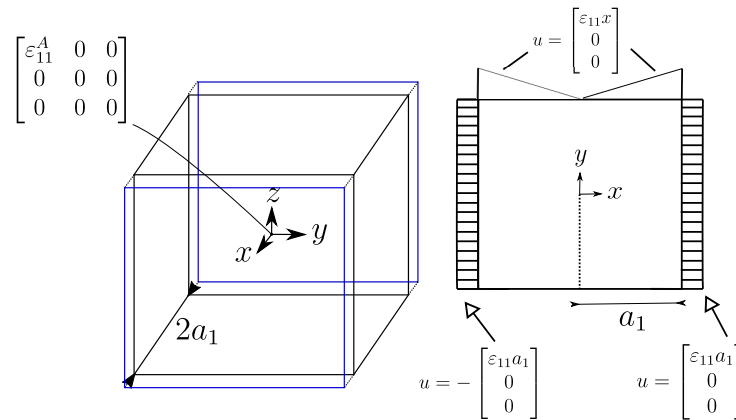


Figure 4. Boundary conditions scheme for a pure-extension state

2.3 Stiffness Tensor and Engineering Constants

Let the symbol $\langle \cdot \rangle$ represent a quantity averaged in volume. The stress-strain relationship of averages is

$$\langle \sigma_{ij} \rangle = C_{ij} \langle \varepsilon_{ij} \rangle \quad (3)$$

In the current work, the C_{ij} in eq. (3) is considered with 36 independents terms. Following Zohdi's methodology [12], six independent ε_{ij}^A are applied in the model, as illustrated in Fig. 4, through eq. (2). Each ε_{ij}^A applied in model, used together with eq. (3), generates six linear set of equations. The six ε_{ij}^A cases, consequently, allow the complete computation of C_{ij} terms. Finally, the engineering constants are obtained through the compliance matrix S_{ij} .

3 Results

3.1 Mesh Influence in Stiffness Matrix

Firstly, one evaluates the effect of mesh size in mechanical properties. The finite element analysis was carried out in ANSYS APDL [15], with a 3-D 10-Node Tetrahedral Structural Solid element. The mesh is generated by TexGen [9, 11], through a general *seed* parameter, which corresponds to element edge size. The stiffness tensor C_{ij} is obtained as explained in subsection 2.3. The Frobenius norm of C_{ij} is evaluated in each mesh size, represented

¹Nomenclature used by [13]. However, such boundary condition is also called Kinematic Uniform Boundary Conditions (KUBC), as stated in Hazanov [14].

by $|C|$ in Fig. 5. The $|C|$ was normalized by $|C|_{avg}$, which is the average of $|C|$ in computed in reference of all meshes. The largest difference in Fig. 5 is lower than 2.80% among the evaluated meshes. Comparing to $|C|_{avg}$, the largest deviation is 1.52%. Due the small advantage of using the finest meshes, the seed size applied in this study is 0.05.

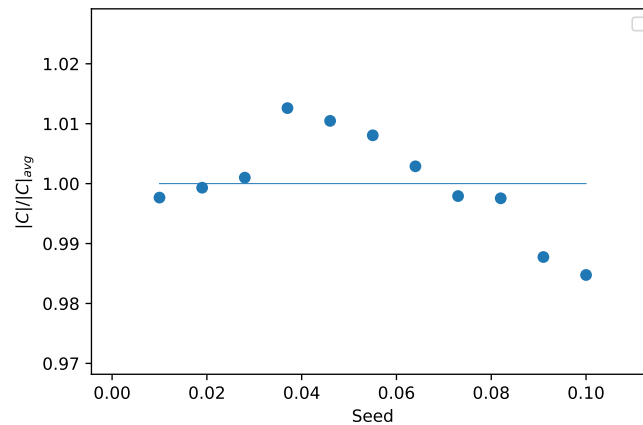


Figure 5. Mesh size influence in stiffness matrix $|C|$

3.2 Comparison with results from literature

The introduced methodology is then compared with Barbero's numerical results [7] and Scida experimental and analytical results [10]. The boundaries conditions applied in this work, as discussed by Espadas [13], over estimated E_1 and E_2 in general, as showed in table 3a and 3b.

Barbero [7] applied periodic boundary conditions (PBC), which is a distinct set of boundary conditions from those applied herein (explained in eq. (2)). PBC estimates the properties of an infinite periodic structure, assuming that both strain and stress are periodic. Such approach requires a full coupling between the degrees of freedom of nodes lying on boundaries, as proposed by Luciano [16]. Another requirement of PBC is mesh periodicity. The main advantage of PBC approach is to simulate strain and stress fields of an infinite body by just modeling one RUC. On other hand, the methodology applied here only imposes a set homogenized strains fields without any periodicity requirements. It has a great advantage of using a mesh-free approach in the model, but the results were slightly different from experimental data, as showed in table 3a. However, the model could not reproduce the geometry with precision. The table 2 shows that the current model reached V_m^α with 16.5% of difference from V_m , which influenced the results, as the eq. (1) is not exact.

In contrast, the results from this work showed good agreement with experimental data for *2/2 Twill E-glass twill weave*, as can be see in table 3b. In this particular case, it was possible to reach a V_m^α closer to V_m from experimental data. The geometry, therefore, could be reproduced with quite good accordance with Scida [10] data, leading to a stress distribution that was closer to what is encountered in real woven-fibre.

3.3 Resulting stress fields in woven composite

One of the main advantages of developing a numerical tool to generate the stiffness matrix of a RUC / RVE is the possibility of observing the stresses on the domain. However, rather than evaluating the absolute stress value, it is important to study the stress relationships between resin and strand regions. In both Fig. 6 and Fig. 7 the stress field σ_{xz} in resin increases in regions where the distance between strands decreases. The stresses in this areas are 4 times greater to the center of resin elements group. It is clear that this stress jumps follow the weave pattern, as demonstrated in Fig. 6 and Fig. 7. Such stress increase does also appears in strands elements group. The stresses jumps, however, are less severe ($\sim 200\%$ larger). The maximum stress, in other hand, is dominant in strand elements. In both cases, the stress peak is larger – about 200% – in comparison to the resin elements group.

Table 3. Comparison with experimental and numerical studies

(a) E-glass/vinylester plain-weave				(b) 2/2 twill E-glass/epoxy woven fabric		
Properties	Present work	Barbero [7]	Scida [10]	Properties	Present Work	Scida [10]
E_1 [Gpa]	26.135	24.439	24.8	E_1 [Gpa]	19.223	19.2±0.2
E_2 [Gpa]	26.718	24.534	24.8	E_2 [Gpa]	19.337	19.2±0.2
E_3 [Gpa]	10.872	10.253	8.5	E_3 [Gpa]	8.290	10.92*
G_{12} [Gpa]	5.132	5.515	6.5	G_{12} [Gpa]	3.464	3.6±0.1
G_{23} [Gpa]	3.043	3.151	4.2	G_{23} [Gpa]	2.071	3.78*
G_{31} [Gpa]	3.335	3.159	4.2	G_{31} [Gpa]	2.222	3.78*
ν_{13}	0.366	0.382	0.28±0.07	ν_{13}	0.440	0.33*
ν_{23}	0.305	0.380	0.28±0.07	ν_{23}	0.392	0.33*
ν_{12}	0.141	0.126	0.11±0.01	ν_{12}	0.134	0.13±0.007

* Analytical solution results from Scida [10]

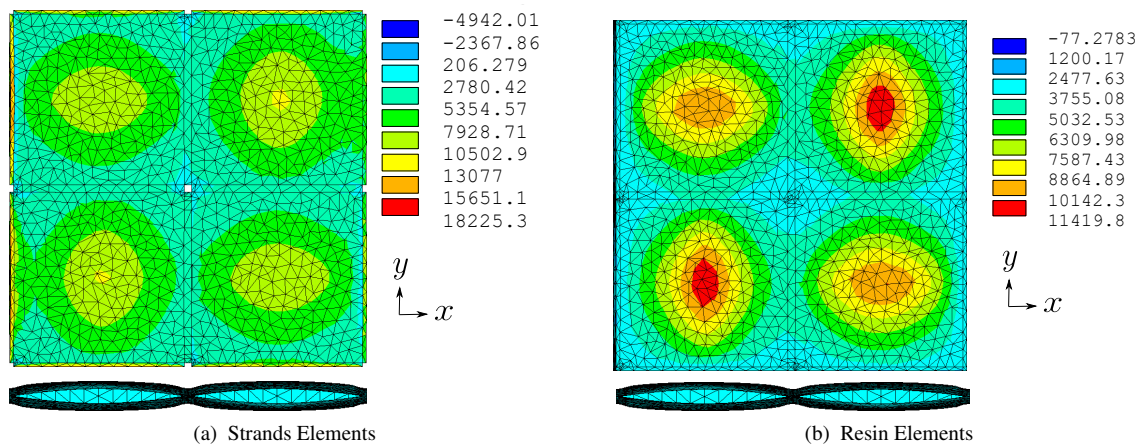


Figure 6. Stress σ_{xz} distributions of E-glass/vinylester plain-weave under ϵ_{xz} strain state

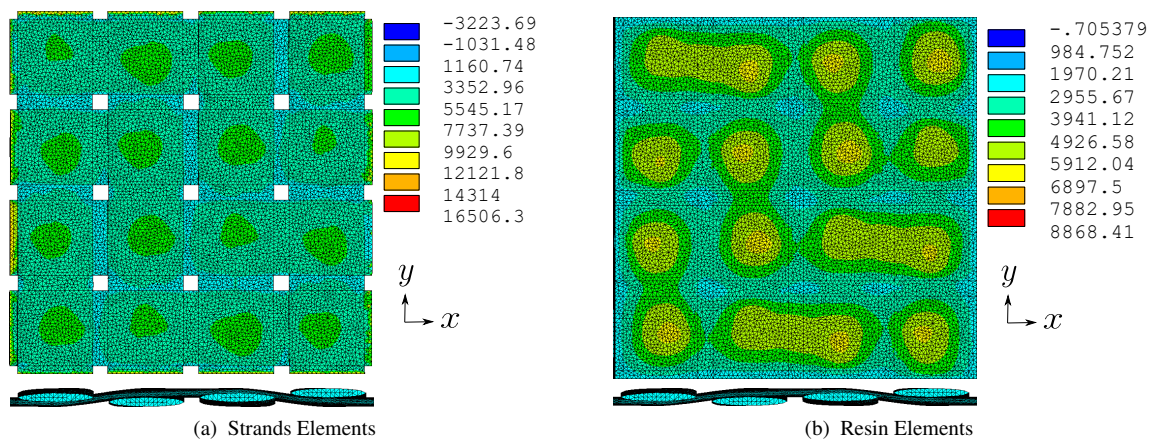


Figure 7. Stress σ_{xz} distributions of 2/2 twill E-glass/epoxy weave under ϵ_{xz} strain state

4 Conclusions

In this article, *Uniform Displacement Boundary Conditions* (UDBC) were applied in order to obtain mechanical properties of two woven-fibre composites: *E-glass/vinylester plain weave* and *2/2 Twill E-glass epoxy weave*. The properties obtained showed good agreement with results from literature. It was verified that both boundary conditions and geometry had influenced the results. Therefore, it must be further investigated how to overcome the difficulty of real woven-fibre geometry representation, as well how others boundaries conditions types can perform the same task. An important point highlighted by the present work is that the use of Classical Laminate Theory hides loss of information that happens due to the reduction of the constitutive tensor, and many analytical models are based on it. In the literature, these models showed good performance for in-plane mechanical properties, although they present inferior performance for out-of-plane properties. As a consequence, further investigation may be carried applying distinct plate theory in analytical models. Namely, first- or higher-order shear deformation plate theories could possibly lead to good results in out-of-plane properties.

Acknowledgements. The authors are grateful to CNPq (Universal project no. 310649/2017-0), CAPES (PROBRAL project no. 88881.198774/2018-01) and DAAD (PROBRAL project no. 57447163) for funding the development of this research.

Authorship statement. The authors hereby confirm that they are the sole liable persons responsible for the authorship of this work, and that all material that has been herein included as part of the present paper is either the property (and authorship) of the authors, or has the permission of the owners to be included here.

References

- [1] Ishikawa, T., 1981. Anti-symmetric elastic properties of composite plates of satin weave cloth. *Fibre Science and Technology*, vol. 15, n. 2, pp. 127–145.
- [2] Ishikawa, T. & Chou, T.-W., 1982a. Elastic behavior of woven hybrid composites. *Journal of composite materials*, vol. 16, n. 1, pp. 2–19.
- [3] Ishikawa, T. & Chou, T.-W., 1982b. Stiffness and strength behaviour of woven fabric composites. *Journal of Materials Science*, vol. 17, n. 11, pp. 3211–3220.
- [4] Sankar, B. V. & Marrey, R. V., 1997. Analytical method for micromechanics of textile composites. *Composites Science and Technology*, vol. 57, n. 6, pp. 703–713.
- [5] Scida, D., Aboura, Z., Benzeggagh, M., & Bocherens, E., 1998. Prediction of the elastic behaviour of hybrid and non-hybrid woven composites. *Composites science and technology*, vol. 57, n. 12, pp. 1727–1740.
- [6] ming Huang, Z., 2000. The mechanical properties of composites reinforced with woven and braided fabrics. *Composites science and technology*, vol. 60, n. 4, pp. 479–498.
- [7] Barbero, E., Trovillion, J., Mayugo, J., & Sikkil, K., 2006. Finite element modeling of plain weave fabrics from photomicrograph measurements. *Composite Structures*, vol. 73, n. 1, pp. 41–52.
- [8] Verpoest, I. & Lomov, S. V., 2005. Virtual textile composites software wisetex: Integration with micro-mechanical, permeability and structural analysis. *Composites Science and Technology*, vol. 65, n. 15-16, pp. 2563–2574.
- [9] Lin, H., Brown, L. P., & Long, A. C., 2011. Modelling and simulating textile structures using texgen. In *Advanced Materials Research*, volume 331, pp. 44–47. Trans Tech Publ.
- [10] Scida, D., Aboura, Z., Benzeggagh, M., & Bocherens, E., 1999. A micromechanics model for 3d elasticity and failure of woven-fibre composite materials. *Composites Science and Technology*, vol. 59, n. 4, pp. 505–517.
- [11] Long, A. & Brown, L., 2011. Modelling the geometry of textile reinforcements for composites: Texgen. In *Composite reinforcements for optimum performance*, pp. 239–264. Elsevier.
- [12] Zohdi, T., 2002. Computational modeling and design of new random microheterogeneous materials. *CISM Course Notes*.
- [13] Espadas-Escalante, J. J., van Dijk, N. P., & Isaksson, P., 2017. A study on the influence of boundary conditions in computational homogenization of periodic structures with application to woven composites. *Composite Structures*, vol. 160, pp. 529–537.
- [14] Hazanov, S. & Amieur, M., 1995. On overall properties of elastic heterogeneous bodies smaller than the representative volume. *International Journal of Engineering Science*, vol. 33, n. 9, pp. 1289–1301.
- [15] Ansys, I., 2018. Ansys @academic research mechanical. vol. Release 18.1.
- [16] Luciano, R. & Sacco, E., 1998. Variational methods for the homogenization of periodic heterogeneous media. *European Journal of Mechanics-A/Solids*, vol. 17, n. 4, pp. 599–617.